Journal of The Electrochemical Society, **153** (9) F199-F204 (2006)
0013-4651/2006/153(9)/F199/6/$20.00 © The Electrochemical Society

Liquid-Injection Atomic Layer Deposition of TiO_x and Pb–Ti–O Films

Takayuki Watanabe,[a,z] Susanne Hoffmann-Eifert,[a] Cheol Seong Hwang,[b,*] and Rainer Waser[a]

[a]*Institute of Solid State Research and CNI—Center of Nanoelectronic Systems for Information Technology, Research Centre Jülich, 52428 Jülich, Germany*
[b]*School of Materials Science and Engineering, Seoul National University, Seoul 151-742, Korea*

Pb–Ti–O films were prepared by liquid-injection atomic layer deposition (ALD) using H_2O as oxygen source after evaluating Ti precursors with different β-diketonate type ligands, $Ti(OC_3H_7)_2(C_{11}H_{19}O_2)_2$ [$Ti(Oi\text{–}Pr)_2(DPM)_2$] and $Ti(OC_5H_{11})_2(C_{10}H_{17}O_2)_2$ [$Ti(Ot\text{–}Am)_2(IBPM)_2$], dissolved in ethylcyclohexane. For both Ti precursors, the apparent thermal activation energy of the deposition rate of TiO_x films increased at a deposition temperature of about 380°C, and the deposition rate of TiO_x films grown at 300°C saturated against the volume of injected Ti precursors. $Ti(Oi\text{–}Pr)_2(DPM)_2$ was selected for the subsequent Pb–Ti–O film deposition because of its high precursor efficiency and the low temperature dependence of the deposition rate. Pb–Ti–O films were prepared using $Ti(Oi\text{–}Pr)_2(DPM)_2$ and $Pb(C_{12}H_{21}O_2)_2$ [$Pb(TMOD)_2$] at deposition temperatures of 240 and 300°C. The deposition rates of Pb and Ti in the Pb–Ti–O process were higher than those in binary PbO and TiO_x processes under the same deposition conditions. The deposition rate of Pb in the Pb–Ti–O process showed a linear increase in response to the injected Pb precursor volume, which was different from the saturated deposition rate of the PbO process. The interface chemistry between the precursors and predeposited cation layers has critical impact on the self-regulated growth mechanism in the multicomponent oxide ALD.
© 2006 The Electrochemical Society. [DOI: 10.1149/1.2219709] All rights reserved.

Manuscript submitted March 1, 2006; revised manuscript received May 17, 2006. Available electronically July 19, 2006.

In order to deposit binary oxide films, such as SiO_2 and Ta_2O_5, onto three-dimensional (3D) nanostructures with a large active area, metallorganic chemical vapor deposition (MOCVD) is widely used because it achieves good step coverage. However, recent studies have indicated a serious issue, namely, that multicomponent oxide films deposited over 3D structures by MOCVD exhibited nonuniformity in cation composition, even if the film thickness appeared to be uniform over the complex structure.[1-3] Therefore, another approach is necessary if uniform coverage of multicomponent oxide films over 3D structures is to be achieved, both in cation composition and in film thickness.

Atomic layer deposition (ALD) is a surface-reaction controlled process. A saturated film growth rate is characteristic to ALD and therefore allows homogeneity to be achieved on complex structures.[4-6] The ALD process utilizes chemisorption on a predeposited layer. It typically consists of a sequential precursor and reactant gas supply, and an appropriate inert gas purge after each step. Purging ensures that any extra precursor that does not directly contribute to the chemisorption is removed from the film's surface along with extra oxidant and pumped out of the reactor. Hence, with sufficient precursor supply and adequate inert gas purging, conformal film coverage and a high controllability of film thickness, as well as film composition, can be expected even for nonplanar substrates.

In this study, Pb–Ti–O was initially chosen for multicomponent ALD aiming finally for ALD-$Pb(Zr,Ti)O_3$. $PbTiO_3$-based perovskites with large switching charges have been investigated in terms of their integration into ferroelectric random access memories (FeRAMs). Due to the developing reductions in feature size and switching voltage, a conformal deposition of very thin films on 3D capacitor structures was required.[1,2]

Our study starts with an evaluation of two Ti precursors with slightly different ligand structures in terms of the thermal decomposition temperature and the self-regulated deposition rate. Thin films of Pb–Ti–O were then deposited on planar substrates using separate precursor gas supplies for Pb and Ti, respectively. All precursors must have a common deposition temperature in multicomponent oxide ALD. This is known as the ALD window.[4] The precursor with the lowest thermal decomposition temperature used in the multicomponent ALD process determines the maximum process temperature. Concerning combination with other precursors, the higher the thermal decomposition temperature of a precursor is, the more flexible ALD process conditions will be. Hence, estimating the thermal decomposition temperature of each precursor in the binary oxide process gives the first indication of what the process temperature of the subsequent multicomponent ALD will be.

A self-regulated growth of TiO_x films has been reported for various halide and alkoxide Ti precursors such as $TiCl_4$, $Ti(OEt)_4$, and $Ti(Oi\text{–}Pr)_4$. The high decomposition temperature of $TiCl_4$ is attractive in view of the flexible multiprecursor ALD process condition.[7] However, the $TiCl_4$ generates corrosive HCl as a result of a reaction with H_2O, so that the growing film and/or ALD apparatus might be damaged. The alkoxide Ti precursor is noncorrosive, while its thermal decomposition temperature around 300°C is too low.[8] Therefore, a noncorrosive Ti precursor with a high decomposition temperature is required. Widely available Pb precursors are limited to β-diketonate derivatives. Precursors with β-diketonate-type ligands are known as one of the promising precursors for achieving a self-regulated growth rate.[4,6] Hence, noncorrosive Ti precursors with β-diketonate ligands are advantageous in terms of combination with β-diketonate-type Pb precursors. Selecting precursors with a common ligand property may allow a self-regulated stacking growth and a use of a common oxidant.

Chemisorption behavior on a predeposited different cation layer is of particular interest in multicomponent ALD. Comparing the binary oxide process with a single precursor, each constituent cation may show different deposition behavior in the multicomponent process as a result of different surface-layer conditions. Although there are several reports on ALD of multicomponent oxide thin films including $PbTiO_x$,[9-17] deposition rates for each constituent cation in the multicomponent ALD process have not yet been carefully investigated.

Experimental

TiO_x and Pb–Ti–O films were deposited on 1 $in.^2$ $Pt(111)/ZrO_x/SiO_x/Si(100)$ substrates at temperatures ranging from 220 to 420°C. An ALD system equipped with an injection system with four independent liquid precursors and a horizontal gas flow reactor was set up for this study. The discrete precursor injection prevents the precursors prereacting in the gas phase. Due to the narrow selectivity of precursors and the limited thermal stability of the low-vapor-pressure β-diketonate-based precursors, liquid-delivery source injection methods were used. In addition, the precursors dissolved in a common solvent were kept at room tempera-

* Electrochemical Society Active Member.
z E-mail: t.watanabe@fz-juelich.de

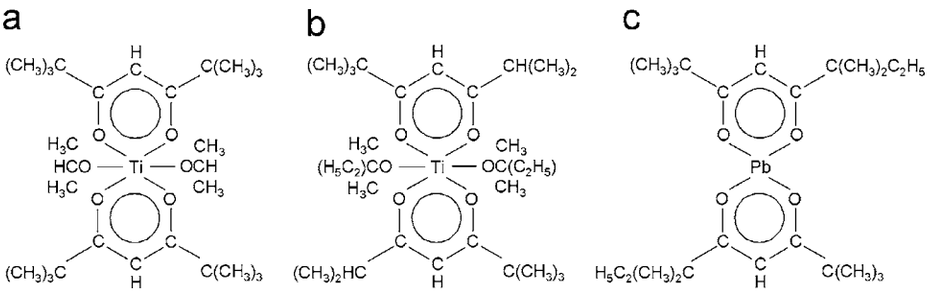

Figure 1. Schematics of (a) $Ti(Oi\text{–}Pr)_2(DPM)_2$, (b) $Ti(Ot\text{–}Am)_2(IBPM)_2$, and (c) $Pb(TMOD)_2$.

ture until they were supplied to the vaporizer. Hence, the liquid injection principle is free from long-term thermal degradation of precursors, which allows the operating lifetime of the precursors to be lengthened in comparison to bubbler-based techniques.

$Ti(Oi\text{–}Pr)_2(DPM)_2$ [$Ti(OC_3H_7)_2(C_{11}H_{19}O_2)_2$, diisopropoxide dipivaloylmethanatotitanium], $Ti(Ot\text{–}Am)_2(IBPM)_2$ [$Ti(OC_5H_{11})_2(C_{10}H_{17}O_2)_2$, ditertiaryamyloxide isobutyrylpivaloylmethanatotitanium], and $Pb(TMOD)_2$ [$Pb(C_{12}H_{21}O_2)_2$, bis(2,2,6,6-tetramethyl-3,5-octanedionato)lead] in ethylcyclohexane (ECH) with a concentration of 0.1 M were used as precursors (see Fig. 1). The solutions were supplied by SAES Getters S.p.A. The injector was opened for a fixed time, and the number of injections per sequence was varied.

Typically, the injector was opened for 1.4–2.0 ms with a frequency of 2 Hz, and 4.0–5.7 μL of precursor was consumed per injection, respectively. The injected precursor was thermally vaporized at 200°C and carried to the horizontal reactor by Ar carrier gas. H_2O gas was used as an oxidant and was supplied for 1 s from a reservoir kept at 10°C. Following the precursor injection and the gas supply of H_2O, the reactor was purged for 5–8 s with 200 sccm Ar gas for all investigations, except the study on purge condition. The reactor pressure was kept at 1 Torr. The deposition rates of the constituent elements and the film composition, as well as the film thickness, were calculated using wavelength dispersive X-ray fluorescence spectroscopy (XRF). The structural properties were analyzed by X-ray diffraction (XRD) and the morphology was studied by means of an atomic force microscope (AFM). The residual C content in the films was measured by X-ray photoelectron spectroscopy (XPS).

Results and Discussion

Evaluation of Ti precursors and optimization of ALD-TiO_x process.— The dependence of the growth rate of TiO_x films on the deposition temperature using $Ti(Oi\text{–}Pr)_2(DPM)_2$ and $Ti(Ot\text{–}Am)_2(IBPM)_2$ as precursors is shown in Fig. 2. The deposition rates increased exponentially with an increasing deposition temperature, and the two straight lines indicate that two thermally activated processes were involved. The apparent activation energies estimated from the gradients of the Arrhenius plots for $Ti(Oi\text{–}Pr)_2(DPM)_2$ and $Ti(Ot\text{–}Am)_2(IBPM)_2$ were 35 and 47 kJ/mol up to a deposition temperature of 380°C, respectively. They then increased to about 120 kJ/mol for higher deposition temperatures. These precursors appeared to start a significant thermal decomposition during film growth at around 380°C.

The deposition rates of the TiO_x films were investigated as a function of the injected precursor volume per cycle at 300 and 360°C, which is below the transition temperature in Fig. 2. As shown in Fig. 3, the deposition rates of the TiO_x films saturated both for the $Ti(Oi\text{–}Pr)_2(DPM)_2$ and the $Ti(Ot\text{–}Am)_2(IBPM)_2$ precursor. Interestingly, differential thermal analysis (DTA) of both precursor powders performed in an Ar gas ambient showed two exothermic peaks at about 270–285°C and 370–410°C.[18] These two peaks originated from a thermal decomposition of the precursors. Hence, the DTA analysis suggests that self-regulated growth occurred even after partial decomposition at around 270–285°C.

From a mass spectrum analysis of the $Ti(Oi\text{–}Pr)_2(DPM)_2$ precursor in a vacuum, it was reported that $Ti(Oi\text{–}Pr)_2(DPM)_2$ starts thermal decomposition at 230°C, while the Ti ion is still connected to the β-diketonate ligand up to around 380°C.[19] At 380°C, a free β-diketonate $[Hdpm\text{-}C(CH_3)_3]^+$ radical was detected and most Ti ions lost the β-diketonate ligand. The thermal decomposition associated with the release of the free β-diketonate radical is probably responsible for the change in the apparent activation energy observed in this study (see Fig. 2). The self-regulated growth rates of the TiO_x films shown in Fig. 3 are obviously related with the perpetuation of the β-diketonate ligand structure at the Ti ion. The partial decomposition of the $Ti(Oi\text{–}Pr)_2(DPM)_2$ at about 280°C appears not to have interfered with the self-regulated growth. The apparent activation energies of the growth rate of TiO_x films at deposition temperatures above and below 380°C are almost in the same regime as the values reported for ALD-SrO from $Sr(DPM)_2$.[16] The values for the apparent activation energy of the SrO film growth increased from 30 to 118 kJ/mol at a deposition temperature of about 380°C.

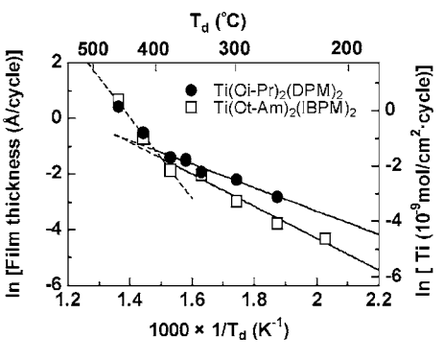

Figure 2. Deposition rate of TiO_x films at various deposition temperatures. During one cycle, 40 μL of 0.1 M $Ti(Oi\text{–}Pr)_2(DPM)_2$ or $Ti(Ot\text{–}Am)_2(DPM)_2$ precursors were injected into the vaporizer.

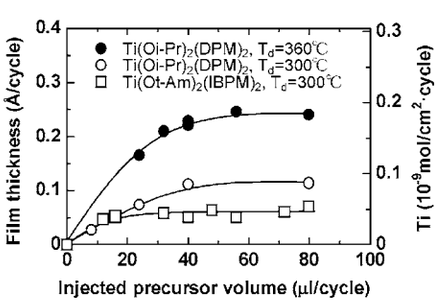

Figure 3. Deposition rate of TiO_x films at 300 and 360°C as a function of the injected Ti precursor volume per cycle at 1 Torr. The flow rate of Ar purge gas was 200 sccm.

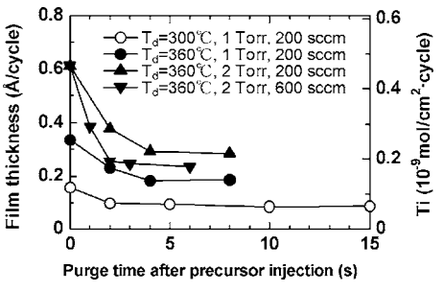

Figure 4. Dependence of the deposition rate of TiO_x films on the purge time after precursor injection at a deposition temperature of 300 and 360°C. For one cycle, 40 μL of 0.1 M $Ti(Oi\text{–}Pr)_2(DPM)_2$ precursor was injected into the vaporizer. Purge times after H_2O supply were 8 and 5 s for deposition temperatures of 300 and 360°C, respectively.

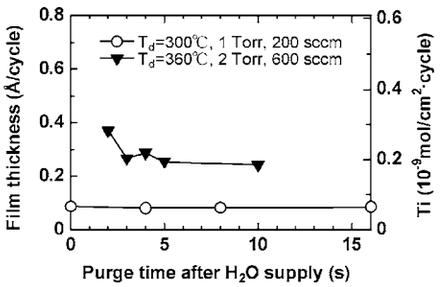

Figure 5. Effect of the purge time after H_2O supply on the deposition rate of TiO_x films at deposition temperatures of 300 and 360°C. Purge times after precursor injection was 8 and 2 s for deposition temperatures of 300 and 360°C, respectively.

At a deposition temperature of 300°C, the deposition rate of TiO_x films saturated at about 0.1 Å/cycle for the $Ti(Oi\text{–}Pr)_2(DPM)_2$ precursor, and the efficiency of the $Ti(Oi\text{–}Pr)_2(DPM)_2$ precursor was enhanced by increasing the deposition temperature. This result indicates that the deposition rate is associated with the chemisorption, which is promoted by thermal energy. For $Ti(Ot\text{–}Am)_2(IBPM)_2$, the deposition rate of the TiO_x films at 300°C saturated at 0.05 Å/cycle. The dimensions of the precursor molecule, the density of the adsorption sites, and the thermal energy required for the chemisorption all affect the saturated deposition rate. The dimensions of the precursor molecule are decisive for a steric hindrance. The deposition rate of TiO_x films using $TiCl_4$, $Ti(OEt)_4$, and $Ti(Oi\text{–}Pr)_4$ depends on the radii of precursor molecules.[20] A smaller Ti precursor molecule gave a higher deposition rate, ranging from 0.3 to 0.56 Å/cycle. Comparing with this value, the present deposition rate of TiO_x films, e.g., 0.1 Å/cycle at a deposition temperature of 300°C using $Ti(Oi\text{–}Pr)_2(DPM)_2$, is low. The present precursor could be partially decomposed at this deposition temperature as described before, but the dimension of the precursor might be larger than the above halide and alkoxide precursors due to the large β-diketonate ligand. Hence, the low deposition rate of TiO_x using Ti precursors with β-diketonate ligand can be ascribed to the molecule radii. As can be seen in Fig. 2, the ALD process using $Ti(Oi\text{–}Pr)_2(DPM)_2$ and that using $Ti(Ot\text{–}Am)_2(IBPM)_2$ are both under thermal chemisorption limitations with an assumption of no oligomerization of the precursors, which means that there are sufficient adsorption sites. Additionally, both of the precursors have a similar ligand structure. Consequently, it can be concluded that $Ti(Ot\text{–}Am)_2(IBPM)_2$ requires a higher thermal energy for the chemisorption on the predeposited Ti–O layer than $Ti(Oi\text{–}Pr)_2(DPM)_2$. The lower activation energy of $Ti(Oi\text{–}Pr)_2(DPM)_2$ compared to $Ti(Ot\text{–}Am)_2(IBPM)_2$ in the ALD regime is advantageous for the uniform coverage of a 3D structure, because there could be a small temperature gradient over the complex structure. The high deposition rate of TiO_x films given by $Ti(Oi\text{–}Pr)_2(DPM)_2$ is also promising for saving process time and precursor consumption. As a result, it was decided that we would only investigate $Ti(Oi\text{–}Pr)_2(DPM)_2$ in detail.

Figure 4 shows the impact that the purge cycle has after the $Ti(Oi\text{–}Pr)_2(DPM)_2$ precursor injection. An insufficient purge cycle can lead to physisorbed precursor molecules remaining on a chemisorbed layer which may be oxidized during the H_2O pulse that follows, thereby preventing self-regulated growth. At a deposition temperature of 300°C, the deposition rate reached a constant value for a purge time of more than 2–4 s. In addition, we investigated the effect of the reactor pressure on the purge behavior at a deposition temperature of 360°C, utilizing high precursor efficiency. Increasing the reactor pressure from 1 to 2 Torr by reducing the pumping speed increased the settled deposition rate from about 0.2 to 0.3 Å, but it did not significantly change the purge time required for reaching a constant deposition rate.

However, hydrodynamic considerations would lead one to expect that the reactor pressure would affect the purge time after both precursor injection and H_2O supply because concentrations of precursor and H_2O molecules in the gas phase and the purge gas flow rate are dependent on reactor pressure. The increment in the deposition rate with increasing reactor pressure at 2 Torr could be ascribed to a purge failure after the H_2O was supplied because of increased partial pressure of H_2O and a slower purge gas flow rate in the reactor compared to the condition at 1 Torr. In this case, the reactor pressure was increased from 1 to 2 Torr simply by decreasing the pumping speed. Thus, the total amount of H_2O molecule moved from the reservoir by its own vapor pressure is lower, while the partial pressure inside the reactor is increased. In this situation, the remaining H_2O acts as a reactive site on the surface, which caused the deposition rate of TiO_x to increase. Subsequently, the purge gas flow rate was increased from 200 to 600 sccm, keeping the reactor pressure at 2 Torr. As a result, the settled deposition rate decreased and the purge time for a constant deposition rate was halved. As is shown later, the purge condition after the H_2O gas supply is sufficient at this time. However, the settled deposition rate is still about 20% higher than the rate observed at 1 Torr. Comparing to the previous condition with purge gas flow rate of 200 sccm at 2 Torr, the partial pressure of H_2O in the reactor at the H_2O pulse turn will be decreased because the Ar gas flow rate was increased to 600 sccm keeping the reactor pressure constant. The slightly higher deposition rate at 2 Torr than that rate observed at 1 Torr may suggest that the partial pressure of H_2O was still increased comparing to the atmosphere at 1 Torr. A reduced desorption of the precursor molecule from the surface is another scenario to explain the slightly higher deposition rate. The desorption rate is expected to decrease at the high pressure ambient, resulting in a high growth rate.

In turn, the effect of the purge time after H_2O gas supply on the deposition rate was investigated at 300 and 360°C under a reactor pressure of 1 and 2 Torr with an Ar purge gas flow of 200 and 600 sccm. As can be seen in Fig. 5, the deposition rate was independent of the purge time at a deposition temperature of 300°C and a reactor pressure of 1 Torr. Here, the gas flow is fast enough for exchanging the gas ambient inside the reactor without leaving H_2O inside the reactor. At a deposition temperature of 360°C and a reactor pressure of 2 Torr, Ar purging for 3 s was necessary to remove the residual H_2O.

Pb–Ti–O film deposition.— For the subsequent deposition of the Pb–Ti–O film we chose $Pb(TMOD)_2$ and $Ti(Oi\text{–}Pr)_2(DPM)_2$ dissolved in ECH as precursors. In our previous study,[21] we found that the thermal decomposition temperature of $Pb(TMOD)_2$ was higher than that of $Pb(DPM)_2$. $Pb(TMOD)_2$ started thermal decomposition at around 320°C in the same experimental procedure that was used

for Ti precursors outlined above. A saturated deposition rate was observed for PbO films with a precursor injection rate above 40 μL/cycle at deposition temperatures of 240 and 300°C. Although the deposited PbO films had edge exclusions in their film thickness, i.e., the PbO film at the center part of the substrates was roughly twice as thick as that at the edge part, with a stable chemisorption onto the Ti–O layer, a self-regulated deposition of the Pb–O layer was still expected. In the case of Pb–Ti–O, the Pb precursor meets with a predeposited Ti–O layer and as a result has a different adsorption mechanism than the binary PbO process. Therefore, we used $Pb(TMOD)_2$ for Pb–Ti–O in combination with $Ti(O\textit{i}\text{–}Pr)_2(DPM)_2$ to probe the interaction between the $Pb(TMOD)_2$ and the Ti–O layer on the one side and between the $Ti(O\textit{i}\text{–}Pr)_2(DPM)_2$ and the Pb–O layer on the other side. ALD is a process based on the interaction of ligands of a predeposited layer and a supplied precursor molecule. From previous Arrhenius plots for the deposition rate of TiO_x and PbO films as a function of the deposition temperature,[21] the significant thermal decomposition temperature of $Ti(O\textit{i}\text{–}Pr)_2(DPM)_2$ and $Pb(TMOD)_2$ precursors was estimated to be 380 and 320°C, respectively. This temperature corresponds to a change from the ALD mode to the CVD mode characterized by a thermal decomposition of the precursor. Naturally, the maximum deposition temperature for a multicomponent ALD process is limited to the lowest thermal decomposition temperature of all the precursors used in the process, because the substrate temperature cannot be varied during the process. Therefore, the maximum deposition temperature of the Pb–Ti–O process is 320°C, i.e., the decomposition temperature of the $Pb(TMOD)_2$ precursors. In this study, Pb–Ti–O films were deposited at 240 and 300°C.

In a unit Pb–Ti–O sequence, the above-described Ti–O cycle was repeated for 4 or 6 times against 1 Pb–O cycle in order to adjust the film composition with a sufficient precursor injection for the saturated deposition rate in the ALD-TiO_x process. Figure 6a shows the mole area density of deposited Pb and Ti in the Pb–Ti–O films and of Pb in the PbO films grown at a deposition temperature of 300°C as a function of the injected Pb precursor volume in one cycle. Here, the binary metal oxide deposition cycle ratio (Ti–O)/(Pb–O) was set to 4.

Because the first layer deposited on the substrate often affects the nucleation process and the ensuing film growth,[22] two sequences beginning with Ti injection or Pb injection were therefore carried out. The unit sequences repeated for the Pb–Ti–O processes were $4 \times [Ti(O\textit{i}\text{–}Pr)_2(DPM)_2\text{–}H_2O] - 1 \times [Pb(TMOD)_2\text{–}H_2O]$ and $1 \times [Pb(TMOD)_2\text{–}H_2O] - 4 \times [Ti(O\textit{i}\text{–}Pr)_2(DPM)_2\text{–}H_2O]$ named Ti and Pb starts, respectively. The deposition rate of Pb roughly doubled in the Pb–Ti–O process compared to the corresponding binary PbO process. As the injected Pb precursor volume in one sequence increased, the deposition rate of Pb increased linearly after an initial abrupt increase, while the deposition rate of Ti was found to be independent of the Pb precursor amount at about 1.0×10^{-9} mol/cm^2 for 4 Ti–O cycles. An equivalent mole area density of 1.0×10^{-9} mol/cm^2 was calculated for a (100) plane of an ideal $PbTiO_3$ single crystal, whose lattice parameter is typically 0.4 nm. Although the deposited films were amorphous as described later, the laminate deposition around the stoichiometric composition is comparable to a layer-by-layer growth of a $PbTiO_3$ crystal with respect to the mole area density of the constituent cation. The deposition rate of the Pb–Ti–O film (Pb/Ti = 1:1) was estimated from the film thickness measured by transmission electron microscopy and the total sequence number. The deposition rate was about 0.5 nm/sequence, which was close to the lattice parameter of the $PbTiO_3$ crystal. The average deposition rate of Ti in the Pb–Ti–O process, 2.5×10^{-10} mol/cm^2 per 1 Ti–O cycle, was approximately 3 times higher than that in the TiO_x process for the same volume of injected precursor. Interestingly, the starting layer on the Pt substrate, either Ti–O or Pb–O, had a negligible effect on the growth

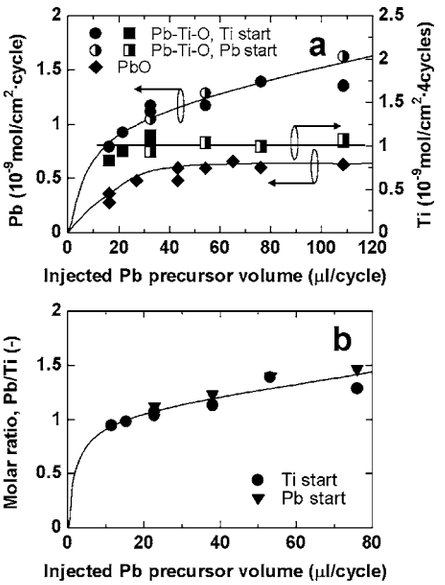

Figure 6. (a) Mole area density of Pb and Ti in the Pb–Ti–O and Pb in the PbO processes at a deposition temperature of 300°C. For one Pb–Ti–O film deposition, $4 \times [(Ti\text{–}O)\text{–}H_2O] - 1 \times [(Pb\text{–}O)\text{–}H_2O]$ or $1 \times [(Pb\text{–}O)\text{–}H_2O] - 4 \times [(Ti\text{–}O)\text{–}H_2O]$ was repeated 40 times. During one Ti–O cycle in the Pb–Ti–O process, 40 μL of $Ti(O\textit{i}\text{–}Pr)_2(DPM)_2$ precursor was injected into the vaporizer. For the PbO film deposition, the $(Pb\text{–}O)\text{–}H_2O$ cycle was repeated 100 times. Purge times after precursor injection and H_2O supply were 5–10 and 8 s, respectively. (b) Pb/Ti molar ratio of the Pb–Ti–O films.

rate and the composition of the resulting Pb–Ti–O films. The following scenarios were considered in an attempt to explain the observed changes in growth behavior.

First, we look at the higher deposition rates of Pb and Ti in the Pb–Ti–O process in comparison to the binary processes. On the growing film surface, the Pb–O and Ti–O layers could have a higher adsorption site density for $Ti(O\textit{i}\text{–}Pr)_2(DPM)_2$ and $Pb(TMOD)_2$, respectively, in comparison to their binary processes. In addition, the Ti–O layer may have a different ligand structure from that in the ALD-TiO_x process as a result of the chemisorption reaction with a Pb–O layer. This may affect the deposition rate of the subsequent Ti–O layers deposited in order to adjust the film composition. Simultaneously, the chemisorption at the heterointerface may occur with a smaller thermal energy than was required in the binary processes. All of these mechanisms can enhance the deposition rates of Pb and Ti in the Pb–Ti–O process.

Second, we discuss the nonsaturation of the Pb deposition rate. The deposition rate of Pb in the Pb–Ti–O process continued to increase with the volume of injected Pb precursor, which was in contrast to the saturated deposition rate observed for the binary PbO process. One possible explanation could be that purging failed to remove residual Pb precursor. However, this was not the case here because when the purge time was extended after $Pb(TMOD)_2$ injection, the nonsaturation of the Pb deposition rate did not change. The Ti–O layer could have more adsorption sites for the Pb precursor than a Pb–O layer, as mentioned above. This probably contributed to the higher deposition rate of Pb in the Pb–Ti–O process compared to the PbO process, particularly in the small Pb precursor injection regime <30 μL/cycle. Looking at a single-crystal $PbTiO_3$ again, a mole area density of 1.0×10^{-9} mol/cm^2 was expected for an ideal layer-by-layer growth. Therefore, a mole area density of more than 1.0×10^{-9} mol/cm^2 per sequence would indicate that multiple layers are deposited on the surface from a viewpoint of ion packing. In Fig. 6a, the deposition rate of Pb appears to increase linearly with the injected Pb precursor volume after the mole area density of Pb

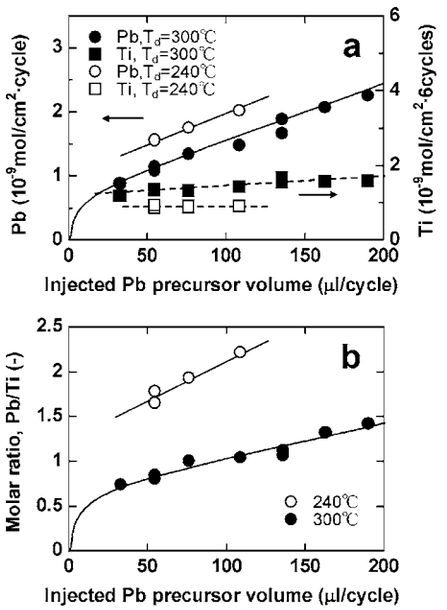

Figure 7. (a) Pb and Ti mole area density per cycle in the Pb–Ti–O films deposited at 300 and 240°C. For the Pb–Ti–O preparation, a unit sequence, $6 \times [(\text{Ti–O})\text{–}H_2O] - 1 \times [(\text{Pb–O})\text{–}H_2O]$, was repeated 30 times. During one Ti–O cycle in the Pb–Ti–O process, 50 μL of 0.1 M $Ti(Oi\text{–}Pr)_2(DPM)_2$ precursor was injected into the vaporizer. Purge times after precursor injection and H_2O supply were set to 8 s. (b) Pb/Ti molar ratio of the Pb–Ti–O films.

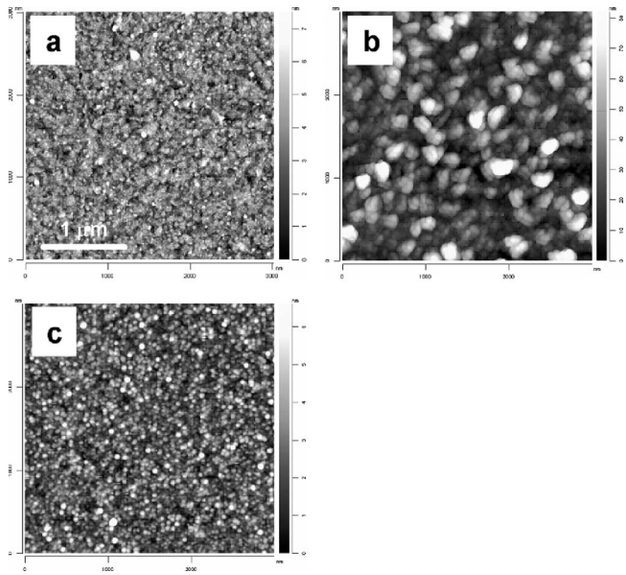

Figure 8. Surface morphology of (a) TiO_x (t = 1.7 nm), (b) PbO (t = 14 nm), and (c) Pb–Ti–O (t = 15.3 nm) films observed by AFM. The films were grown on $Pt/ZrO_x/SiO_x/Si$ substrates at 300°C.

has exceeded 1.0×10^{-9} mol/cm^2. Consequently, we suppose that the underlying Ti–O layer catalyzed the decomposition of the Pb precursor and/or enhanced an oligomerization of the Pb precursor, which might be promoted by increasing the injected precursor volume. Both scenarios would result in the nonsaturated growth rate of the Pb precursor. The Pb/Ti ratio depicted in Fig. 6b increased linearly from 1.0 to 1.5 when the Pb injection volume was increased by a factor of 4 from 20 to 80 μL/cycle, respectively. The Pb/Ti ratio over 1.0 reveals that multiple Pb–O layers were deposited in the unit sequence.

Figure 7 shows the mole area density of Pb and Ti and the Pb/Ti ratio as a function of the injected Pb precursor volume in a broad range of injected Pb precursor volumes at two deposition temperatures of 240 and 300°C. The ratio of the binary metal oxide deposition cycle was set to (Ti–O)/(Pb–O) = 6. Again, the deposition rate of Pb did not show any saturation, but rather a linear increase. In accordance with the apparent negative and positive activation energies observed in the binary PbO and TiO_x processes,[21] the deposition rates of Pb and Ti were increased and decreased, respectively, by changing the deposition temperature from 300 to 240°C. At a deposition temperature of 300°C, a certain increase in the deposition rate of Ti was confirmed when the volume of injected Pb precursor was extensively changed. We believe that this is due to the increased number of adsorption sites on the PbO surface as a result of a greater amount of adsorbed Pb–O. The negligible increase in the deposition rate of Ti at 240°C could be due to the less active adsorption reaction at this temperature.

In addition to the study of growth behavior, we investigated the crystallinity, surface morphology, and residual C content in the as-deposited films. The PbO and TiO_x films deposited at 300°C were crystallized and amorphous, respectively. For the Pb–Ti–O films deposited under the present conditions, no diffraction peaks originating from a crystalline $PbTiO_3$ phase could be detected. Figure 8 shows the surface morphology in a 3×3 μm array of TiO_x, PbO, and Pb–Ti–O films deposited at 300°C as observed by AFM. The TiO_x film, which is considered to be amorphous, showed no particular grain structure, while a significant granular surface structure was confirmed for the PbO film. The values of the root-mean-square surface roughness (R_{rms}) of the TiO_x, and PbO films were 1.5 and 16.8 nm, respectively. The Pb–Ti–O films grown in a process that combined the two binary processes showed a fine granular-shaped structure with an R_{rms} of 1.1 nm. The R_{rms} of the Pt-covered Si substrate was 0.9 nm. The residual C content in the Pb–Ti–O film prepared at 300°C was characterized by XPS after 1 min sputtering to remove surface adsorbates. The Pb–Ti–O film contained only 2% of C in spite of the low deposition temperature. In the case of low-temperature MOCVD, a considerable amount of residual C of more than 15% is sometimes detected in the films.[23] In the present study, the deposition temperature was kept low in order not to decompose the precursor, and no oxidant that promotes the decomposition of the precursor was supplied during the precursor injection. These experimental conditions may cause one to expect a large amount of residual C content in the film. Nevertheless, the present low C content reveals that the majority of C included in the ligands was removed from the film's surface by interactions with either the H_2O pulse or a subsequent precursor pulse. Post-ALD annealing for crystallization can further decrease the residual C content.

Conclusions

Two liquid precursors of $Ti(Oi\text{–}Pr)_2(DPM)_2$ and $Ti(Ot\text{–}Am)_2(IBPM)_2$ dissolved in ethylcyclohexane were evaluated for use in liquid-injection ALD. TiO_x films prepared using the two precursors showed a saturated deposition rate against the volume of injected Ti precursor at a deposition temperature of 300°C. Although the observed thermal decomposition temperatures for the precursors were comparable, the lower activation energy and higher saturated deposition rate of $Ti(Oi\text{–}Pr)_2(DPM)_2$ compared to $Ti(Ot\text{–}Am)_2(IBPM)_2$ was found to be advantageous for the subsequent multicomponent ALD process. Pb–Ti–O films were prepared using $Ti(Oi\text{–}Pr)_2(DPM)_2$ and $Pb(TMOD)_2$ at deposition temperatures of 240 and 300°C. In the Pb–Ti–O process, the deposition rate of Pb showed a linear increase with respect to the injected Pb precursor volume, which was different from the saturated deposition rate of the PbO process. The deposition rates of Pb and Ti in the Pb–Ti–O process were more than twice as high as those in the binary PbO and TiO_x processes. It was therefore concluded that the

interface chemistry between the precursors and the predeposited cation layer has a critical impact on the self-regulated growth rate in the multicomponent oxide ALD process.

Acknowledgments

The authors thank Dr. A. Besmehn for XPS analysis, W. Krumpen for XRF analysis, M. Gebauer and M. Gerst for their technical support, and L. Cattaneo, S. Carella (SAES Getters S.p.A), and Dr. Y. Tasaki (Toshima MFG Co., Ltd.) for fruitful discussions. SAES Getters S.p.A is gratefully acknowledged for supplying the precursors. One of the authors (T.W.) also extends thanks to the Alexander von Humboldt Stiftung (A.vH.) for awarding him a research fellowship. This collaboration with C.S.H. was supported by A.vH.

Research Center Juelich assisted in meeting the publication costs of this article.

References

1. A. Nagai, J. Minamidate, G. Asano, C. J. Choi, C.-R. Cho, Y. Park, and H. Funakubo, *Electrochem. Solid-State Lett.*, **9**, C15 (2006).
2. A. Nagai, G. Asano, J. Minamidate, C. J. Choi, C.-R. Cho, Y. Park, and H. Funakubo, *Mater. Res. Soc. Symp. Proc.*, **830**, D2.2 (2005).
3. C. S. Hwang, S. Y. No, J. Park, H. J. Kim, H. J. Cho, Y. K. Han, and K. Y. Oh, *J. Electrochem. Soc.*, **149**, G585 (2002).
4. L. Niinistö, J. Päiväsaari, J. Niinistö, M. Putkonen, and M. Nieminen, *Phys. Status Solidi A*, **201**, 1443 (2004).
5. H. Kim, *J. Vac. Sci. Technol. B*, **21**, 2231 (2003).
6. R. L. Puurunena, *J. Appl. Phys.*, **97**, 121301 (2005).
7. M. Ritala, M. Leskelä, E. Nykänen, P. Soininen, and L. Niinistö, *Thin Solid Films*, **225**, 288 (1993).
8. V. Pore, A. Rahtu, M. Leskelä, M. Ritala, T. Sajavaara, and J. Keinonen, *Chem. Vap. Deposition*, **10**, 143 (2004).
9. H. Seim, H. Mölsä, M. Nieminen, H. Fjellvåg, and L. Niinistö, *J. Mater. Chem.*, **7**, 449 (1997).
10. M. Vehkamäki, T. Hänninen, M. Ritala, M. Leskelä, T. Sajavaara, E. Rauhala, and J. Keinonen, *Chem. Vap. Deposition*, **4**, 227 (1998).
11. M. Vehkamäki, T. Hatanpää, T. Häanninen, M. Ritala, and M. Leskelä, *Electrochem. Solid-State Lett.*, **2**, 504 (1999).
12. M. Schuisky, K. Kukli, M. Ritala, A. Hårsta, and M. Leskelä, *Chem. Vap. Deposition*, **6**, 139 (2000).
13. M. Nieminen, T. Sajavaara, E. Rauhala, M. Putkonen, and L. Niinistö, *J. Mater. Chem.*, **11**, 2340 (2001).
14. M. Nieminen, S. Lehto, and L. Niinistö, *J. Mater. Chem.*, **11**, 3148 (2001).
15. W. C. Shin, S. O. Ryu, I. K. You, S. M. Yoon, S. M. Cho, N. Y. Lee, K. D. Kim, B. G. Yu, W. J. Lee, K. J. Choi, and S. G. Yoon, *Electrochem. Solid-State Lett.*, **7**, F31 (2004).
16. O. S. Kwon, S. K. Kim, M. Cho, C. S. Hwang, and J. Jeong, *J. Electrochem. Soc.*, **152**, C229 (2005).
17. J. Harjuoja, A. Kosola, M. Putkonen, and L. Niinistö, *Thin Solid Films*, **496**, 346 (2006).
18. SAES Getters S.p.A., Private communication.
19. A. E. Turgambaeva, V. V. Krisyuk, S. V. Sysoev, and I. K. Igumenov, *Chem. Vap. Deposition*, **7**, 121 (2001).
20. M. Ritala, M. Leskelä, and E. Rauhala, *Chem. Mater.*, **6**, 556 (1994).
21. T. Watanabe, S. Hoffmann-Eifert, C. S. Hwang, and R. Waser, *Mater. Res. Soc. Symp. Proc.*, **902E**, 0902-T04-07.1 (2006).
22. T. Watanabe and H. Funakubo, *Jpn. J. Appl. Phys., Part 1*, **39**, 5211 (2000).
23. C. Durand, C. Dubourdieu, C. Vallée, E. Gautier, F. Ducroquet, D. Jalabert, H. Roussel, M. Bonvalot, and O. Joubert, *J. Electrochem. Soc.*, **152**, F217 (2005).